ISSN: 2578-7365

Research Article

Journal of Chemistry: Education Research and Practice

# Introduction to NMR Spectroscopy for Physical and Analytical Chemistry: The Case of the $BF_4^-$ Anion

**Włodzimierz Makulski***

*Laboratory of NMR Spectroscopy, Faculty of Chemistry, University of Warsaw Pasteura Poland*

***Corresponding Author**
Włodzimierz Makulski, Laboratory of NMR Spectroscopy, Faculty of Chemistry, University of Warsaw Pasteura, Poland.

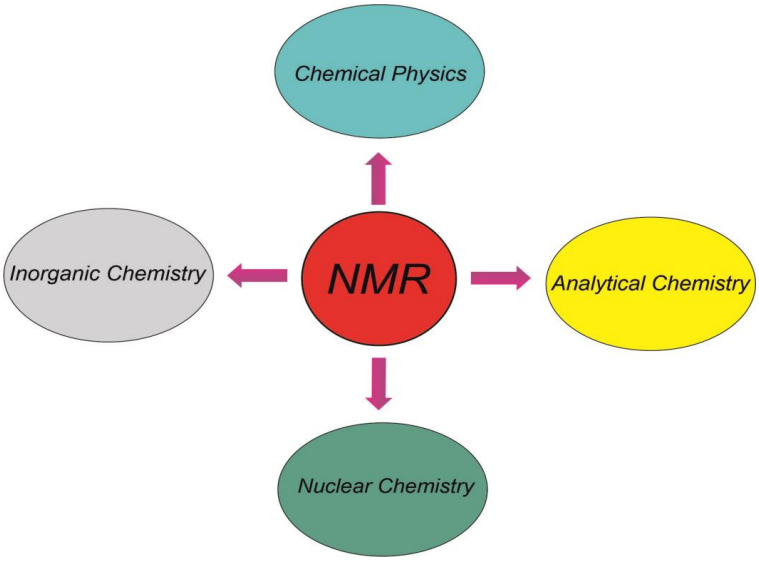
**Submitted:** 2026, Sep 03; **Accepted:** 2026, Oct 23; **Published:** 2026, Oct 28

**Citation:** Makulski, W. (2026). Introduction to NMR Spectroscopy for Physical and Analytical Chemistry: The Case of the BF4- Anion. *J Chem Edu Res Prac, 10*(2), 01-11.

**Abstract**

*Simple 1D NMR measurements of an inorganic compound ($NaBF^4$) in a water solution were proposed as an undergraduate exercise in the chemistry course. 19F NMR chemical shifts were measured in dilute aqueous solutions of tetrafluoro borate salts. The 11B/10B secondary isotope effect on the $^{19}F$ chemical shift was stated as $^1\Delta\delta^{19}F(^{11}B,^{10}B)$=-0.053 ppm. The peak integrations indicated an abundance of $^{11}B$ (80.18%) and $^{10}B$ (19.82%) in the current natural boron-containing salt. Spin-spin coupling constants $^1J(^{19}F,^{10}B)$= ~ 0.53 Hz and $^1J(^{19}F,^{11}B)$= ~ 1.55 Hz were found using the convolution procedure. Several additional properties of water solutions were given: $^{19}F$ nuclear relaxation times, hydrolysis of $BF_4^-$ anions, spin-spin nuclear magnetic couplings, and nuclear magnetic moments of boron isotopes. $^{10/11}B$ abundance measurements using mass spectrometry (MS) were also included and briefly described.*

**Keywords:** Tetrafluoroborate, NMR Spectra, Nuclear Magnetic Shifts, Spin-Spin Coupling Constants, MS Spectra




**Scheme 1:** Graphical Abstract: NMR experimental research of different chemical branches.

## 1. Introduction

NMR spectroscopy plays an essential role in addressing a wide range of chemical problems. It is typically used to interpret chemical structures and processes in organic chemistry, where sets of chemical shifts ($^{1}H$, $^{13}C$, and $^{15}N$) and spin-spin couplings are required to characterize new products. However, it is essential to remember that the first NMR spectra were recorded for inorganic species dissolved in water solutions. In this paper, we present a set of NMR spectra designed to analyze the main spectral parameters: chemical shifts, spin-spin coupling constants, and integrated values of particular resonance signals. Many topics related to this issue are essential for inorganic, physical, analytical, and nuclear chemistry and can be tested in each NMR laboratory in a relatively short time of ~ 3÷4 hours. It provides a concise introduction to the physical principles and practical instrumentation for recording and interpreting NMR spectra. The subject of this research is the tetrafluoroborate anion, $BF_4^-$, a well-known and widely used inorganic salt. $BF_4^-$ is a weakly coordinating anion, which can slightly hydrolyze in water solutions. From an NMR point of view, the anion must have a strictly tetracoordinated structure, with an electric field gradient close to zero, and boron signals exhibit long relaxation times and sharp resonance peaks.

The $^{19}F$ nucleus, with spin ½ and 100% natural abundance, has high sensitivity, comparable to that of proton ($^{1}H$), and is readily observed on most spectrometers. Because of the similarity of $^{1}H$ and $^{19}F$ frequencies, the resonance probe-heads can be tuned to both nuclei, and no special equipment is needed. The boron isotope effect on chemical shift is readily observed in $^{19}F$ NMR spectra. The key to this experiment is to determine the natural abundance of boron isotopes from the integrals of two separate $^{19}F$ NMR signals. Two signals from $^{10}BF_4^-$ and $^{11}BF_4^-$ anions are dispersed by ~0.053 ppm and can be recorded with a high signal-to-noise ratio over a short period. The spin-spin splittings of $^{11}B/^{10}B$-$^{19}F$ can also be seen. These values are strongly dependent on solution concentrations. The most fundamental physical properties of specified nuclei are shown in Table 1.

During the discussion of our experiment, we have tried to convey the physical essence and perception of the individual phenomena associated with each nuclear magnetic resonance. The role of the lock system, tuning and shimming processes, pulse sequences, Fourier transformation, and spectral manipulation will be discussed.

| | $^{1}H$ | $^{19}F$ | $^{11}B$ | $^{10}B$ |
|---|---|---|---|---|
| Spin | 1/2 | 1/2 | 3/2 | 3 |
| Natural Abundance/% | 99.9845 | 100 | 81.4 | 19.6 |
| Quadrupole moment, Q(b) | 0.00 | 0.00 | +0.0407(3) | +0.0847(6) |
| Chemical shift range, ppm | -1÷12 | -300÷400 | -100÷100 | -100÷100 |
| Larmor frequency at 11.74T | 500.606 | 470.969 | 160.614 | 53.784 |
| Reference compound | TMS | $CFCl_3$ | $BF_3{\cdot}OEt_2$ | $BF_3{\cdot}OEt_2$ |
| Relative receptivity to $^{1}H$ | 1.00 | 0.830 | 0.165 | $3.96{\cdot}10^{-3}$ |

**Table 1: NMR parameters of $^{1}H$, $^{19}F$, $^{11}B$, and $^{10}B$ nuclei**

This article is primarily intended for teachers who introduce basic NMR concepts to students in the first three years of study in fundamental Chemical Physics, Inorganic and Analytical Chemistry, or Nuclear Chemistry courses. The experiment presented here was conducted in the Department of Chemistry at Warsaw University over the last 10 years and has an excellent reputation among students.

## 2. The Development of the Workshop

We performed the experimental measures in small groups of between two and six people. We began with a brief written colloquium lasting approximately 30 minutes. The test questions should assess basic knowledge of NMR spectroscopy [1,2,3]. Students were told to read the lab instructions carefully and to be familiar with the basic principles of NMR spectroscopy. Obviously, for preparation, they had access to the public internet and library resources. In our Metrological Lab (Department of Chemistry), we have two spectrometers: a Varian-INOVA/Agilent 500 MHz and a Bruker-AVANCE 500 MHz. The Varian-INOVA spectrometer system is not fully automated and requires direct operator intervention. It is much more didactic and instructive for students. The necessary actions are shortly described below.

### 2.1. Sample Preparation

Experiments performed on high-resolution NMR spectrometers use thin-walled glass tubes (Wilmad, Norell) with high precision. In our case, the 5 mm o.d. Wilmad-528PP tube was selected, which is suitable for measurements at 11.74T. A small amount (10-50 mg) of sodium tetrafluoroborate $NaBF_4$ (Sigma-Aldrich, 98%) powder was dissolved in 1mL of heavy water (99.9 % $D_2O$, Cambridge I.L.), and the solution was filtered with a cotton scroll and injected into the NMR test tube. The concentration of tetrafluoroborate was determined to be ~0.2 mol/L. Other salts are also accessible for usage: $LiBF_4$, $NH_4BF_4$, and $KBF_4$.

### 2.2. The Deuterium Lock

The deuterium lock system is needed for the long-term stability of the magnetic field $B_0$. The basis for operating this channel is the observation of the deuterated signal and its comparison with the numerical value of the $^{2}H(D)$ resonance frequency. The

appropriate compensation for any field drift is made a few times in one second. The lock system permits the recording of high-resolution spectra, during which even minor line splitting can be observed. A large number of deuterated compounds are available commercially (Aldrich-Sigma, Cambridge I.L., Eurisotop). Different isotopic enrichments are possible, ranging from 98% to 99.999%. Tetrafluoroborates are very soluble in water-$d_2$, and less soluble in acetonitrile-$d_3$ and acetone-$d_6$. The well-structured signals are obtained only in liquid water (visible multiplets).

### 2.3. Tuning the Probe

Before acquiring any spectrum, it is necessary to adjust the probe to the proper transmitter frequency and the detection-circuit impedance. This is achieved by two capacitors mounted inside the probe near the coils: one operating at the specified frequency ($^{19}$F: 470.969 MHz, $^{11}$B: 163.614 MHz, and 10B: 53.784 MHz) and the other handling the survey circuit's impedance. In our Varian/Agilent spectrometer, this is performed manually using a dedicated counter.

### 2.4. Adjusting the Shims

In the NMR spectrometer, the liquid sample should be tested in a uniform static magnetic field. According to this requirement, the regular field must be adjusted before analysis begins. To ensure a magnetic field, a shimming system that regulates several small coils, known as shims, is necessary. The “shimming” procedure is performed by observing the deuterium resonance signal in the lock channel. Students can participate in this activity to test their potential and intuition by comparing the spectrum obtained from a single scan with the known final spectrum. The spin-spin coupling in the $^{11}$B-$^{19}$F and $^{10}$B-$^{19}$F system pattern can be helpful here.

### 2.5. Pulse Sequence

We perform the simplest NMR experiment using the basic s2pul (single two-pulse) sequence with a single rectangular pulse of ~45° ($\pi/4 = 8$ µs). The meaning of special $\pi/2$, $\pi$, and $2\pi$ pulses can also be observed and discussed. Calibration of NMR pulses can be shown to students who can read it from the computer memory, because of the long time needed to take a full spectral course. Any substance containing short-lived, relaxing 19F nuclei can also be used (e.g., in our lab, gaseous $CH_3F$ and $CHF_3$ are available).

### 2.6. $^{19}$F Relaxation Times (T1)

The screenshot illustrates the relaxation-time measurements discussed in Appendix 1 (see Figures 8 and 9). The difference in relaxation times is caused by distinct quadrupole electric moments of boron nuclei: $^{10}$B (-0.08(7) barn) and $^{11}$B (+0.04059(10) barn). The spectrum from a single pulse is insufficient to produce a high signal-to-ratio image. Usually, we are forced to record 32, 128, or even 256 scans. The final S/N was about 1800/1. Only in this case can the proper signal integration numbers be measured. Figure 1 (below) shows the $^{11}$B/$^{10}$B relations measured for different d1 relaxation times. Correct results are obtained when d1 is sufficiently long to ensure proper nuclear relaxation. Additionally, short, exciting pulses should be possible due to the relatively long relaxation times of fluorine nuclei in $^{10}BF_4^-$ and $^{11}BF_4^-$.

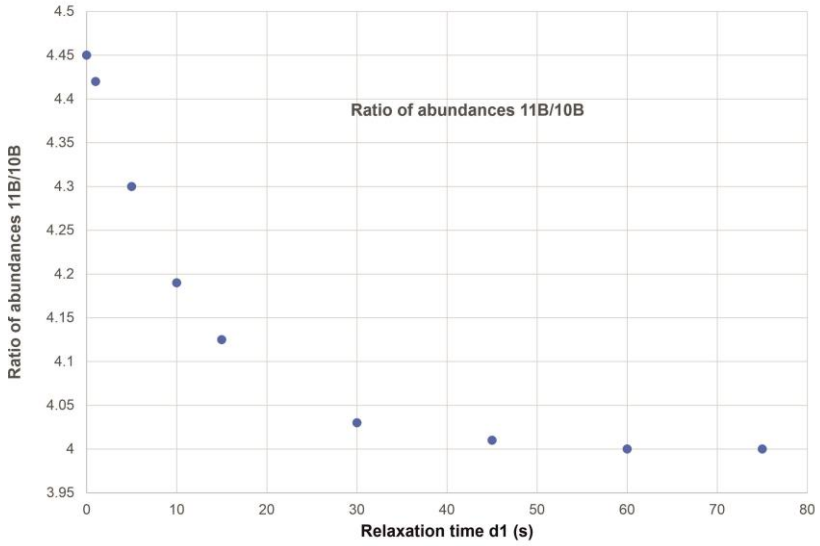



**Figure1:** $^{11}$B/$^{10}$B isotope ratio depending on the d1 relaxation time after the exciting pulse.

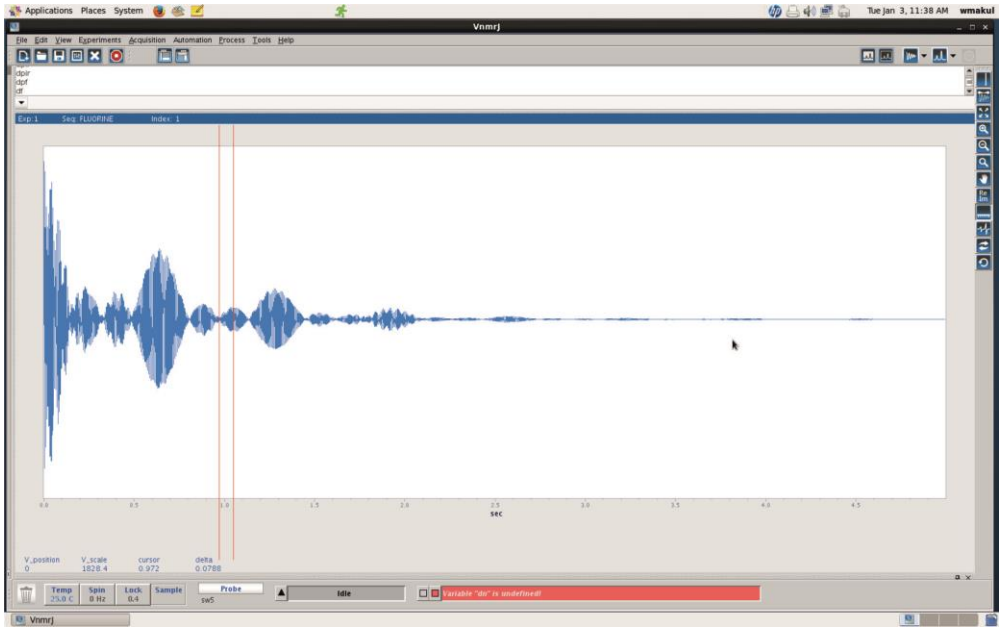


**Figure 2:** Screenshot of the $^{19}F$ FID recorded over 5 s of acquisition time for the $BF_4$ anion

## 2.7. Fourier Transformation

The FID (free induction decay) is shown in Figure 2. The digitalisation of the given spectrum is a consequence of sampling the induced current in the coil detector. It can be visualised when a small fragment of the entire spectrum is observed (see Figure 3). The zero-filing procedure requires applying an fn parameter up to 2×np (the number of points), or even larger.

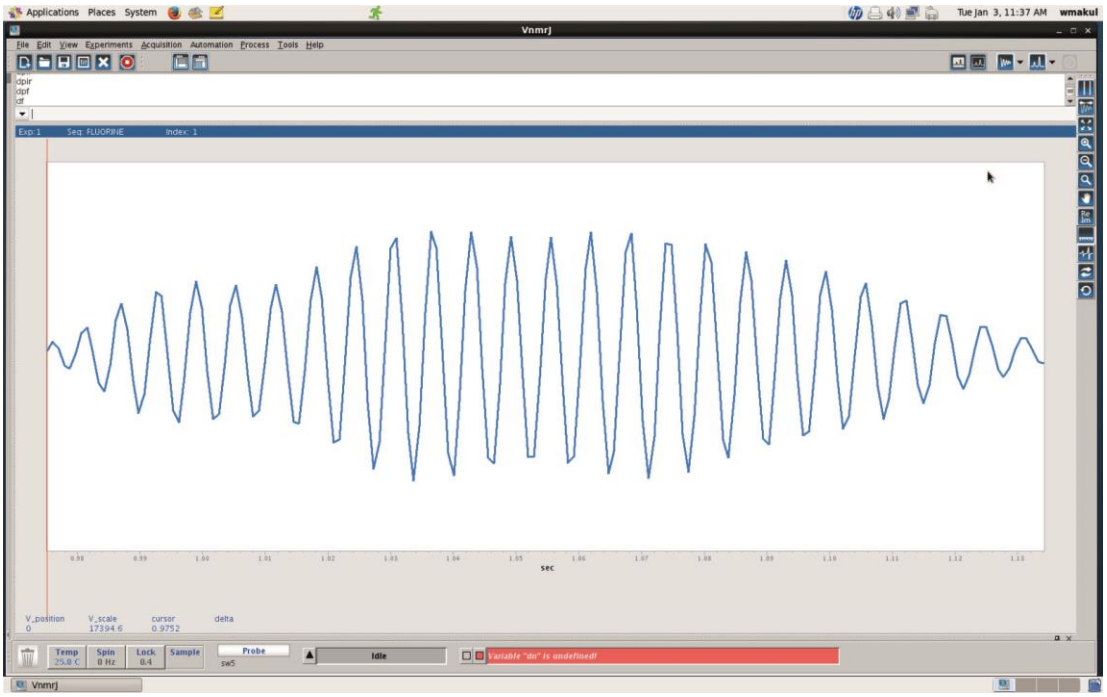


**Figure 3:** Fragment of FID from Figure 2. The digitalisation of the signal induced in the detecting coil is clearly visible.

## 2.8. Manipulation of the Spectrum

Before reading the spectrum parameters, chemical shifts, frequencies, and peak integrations, phase corrections should be applied to remove phase errors. If the integration procedure is implemented, the baseline correction (bc) can be performed. Our spectral background is flat and readily phase-corrected. Automating phasing works also quite well.

## 2.9. Analysis of the Spectrum

The $^{19}F$ NMR spectrum was recorded using 32 scans, with an acquisition time of 5s, a pulse width of 8 µs (45°), and a relaxation delay of 30s (see Figure 4). Measurements of chemical shifts require a reference substance, namely pure liquid $CFCl_3$ for $^{19}F$ NMR (see 2.2). Another form of standardisation is the measurement of a 1% TMS sample in $CDCl_3$ solution and the recalculation of the $CFCl_3$ signal position according to the IUPAC recommendations [4]. Finally, we can read out the main spectral parameters – chemical shifts in ppm, frequencies in "small" Hz, absolute radiofrequencies in MHz, and integration numbers. All these parameters are shown in Table 2.

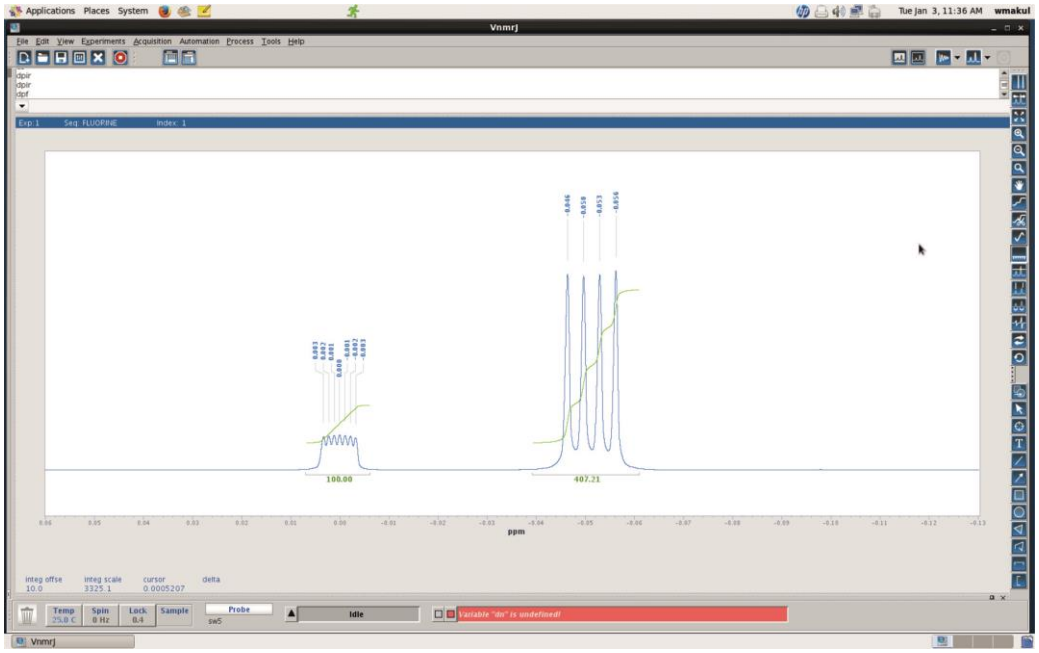



**Figure 4:** 470.592 MHz $^{19}F$ NMR spectrum of 2.0 mol/L solution of $NaBF_4$ in $D_2O$.

The chemical shift is defined in the frequency domain as:

$$\delta = \nu_{sample} - \nu_{reference}/\nu_{reference} = \sigma_{reference} - \sigma_{sample} \quad (1)$$

The appropriate vsample and vreference frequencies are expressed in MHz. A simple correlation with the shielding constant property was also stated. The recalculation of the absolute shielding scale can be discussed in detail with students. The absolute shielding constants of referenced substances should be known here (see 2.3). Susceptibility corrections can be mentioned here. The distance between signals in a given multiplet is called a coupling constant, expressed in Hz. In Figure 4 above, we can see $^1J(^{19}F,^{11}B)$=1.55 Hz and $^1J(^{19}F,^{10}B)$=0.53 Hz. Unlike the chemical shift (δ/ppm), spin-spin coupling is independent of the applied magnetic field but depends on the molecular structure and chemical conditions of the sample. Because $^{19}F$ NMR peaks are not fully resolved, only splitting parameters can be read directly from the spectrum. Nevertheless, convolutional analyses of the line shapes of specific signals yield the correct spin-spin coupling constants. Furthermore, if we acquire $^{11}B$ and $^{10}B$ NMR spectra, which are much better resolved, a simple analysis of the resonance signals can yield reliable spin-spin coupling results (see Figure 5 in §2.1).

It has been found that the $^{19}F$-$^{11}B$ pin-spin coupling varies between 1 and 5 Hz, depending on the concentration and the accompanying cation in a given solution [5]. The intensities in each $^{19}F$ signal are in the ratio 1:1:1:1:1:1:1 ($^{10}BF_4^-$) and 1:1:1:1 ($^{11}BF_4^-$) because of boron spin numbers I = 3 and 3/2, respectively. The quadrupole moments are responsible for line intensity ratios other than for half-integer spins (modified Pascal's triangle). $^1J(^{19}F,^xB)$ spin-spin coupling constants are strongly dependent on the solute concentration and kind of solute used [6]. The $^{19}F$ NMR spectrum illustrates the fundamental parameters of each type of 1D spectrum: chemical shifts, spin-spin coupling constants, and integration values (Figure 4). Due to the isotope effect, we can calculate the abundances of the isotopes in our sample: 19.82% ($^{10}B$) and 80.18% ($^{11}B$), corresponding to the integrals of the areas under the peaks that constitute the multiplets. The $^{11}B/^{10}B$ ratio is 4.045, in good agreement with the literature.

| Peak number | Chemical shift, ppm | Chemical shift, Hz | Radiofrequencies MHz | Integration number, % |
|---|---|---|---|---|
| 1 | 0.003 | 1.54 | 470.96916142 | 19.82 |
| 2 | 0.002 | 1.04 | 470.96916092 | |
| 3 | 0.001 | 0.53 | 470.96916040 | |
| 4 | 0 | 0 | 470.96915988 | |
| 5 | -0.001 | -0.53 | 470.96915935 | |
| 6 | -0.002 | -1.04 | 470.96915884 | |
| 7 | -0.003 | -1.54 | 470.96915834 | |
| 8 | -0.046 | -21.87 | 470.96913801 | 80.18 |
| 9 | -0.050 | -23.41 | 470.96913647 | |
| 10 | -0.053 | -24.96 | 470.96913492 | |
| 11 | -0.056 | -26.50 | 470.96913338 | |
| $^{11}$B and $^{10}$B radiofrequencies:160.6140168 MHz and 53.7833003 MHz, respectively. | | | | |

**Table 2: Results from the 19F NMR Spectrum of Sodium Tetrafluoroborate**

## 3. Final NMR Analyses and Developments.

### 3.1. Inorganic chemistry

The tetrafluorides of Li, Na, and $NH_4$ show excellent solubility in water. Solutions with concentrations ranging from 0.01 to 5 M can be easily prepared. If the NMR analysis is performed a few days after preparation of the salt solute, additional $BF_{4-}$ and boron signals appear in the spectra. All exhibit higher chemical shift values and lower shielding constants and belong to the $BF_3OH^-$ anions. They are a consequence of the hydrolysis of the tetrafluoroborate anions in water and will be discussed in Appendix 3.

Our tetrafluoroborate solution can be used for precise measurements of $^{10}$B and $^{11}$B NMR spectra. The characteristic quintet signals are well resolved, and $^1J(^{19}F,^xB)$ spin-spin coupling constants can be read and compared with those established from $^{19}$F NMR spectra. It is important to note that specific properties of water solutions differ, e.g., relaxation times between light ($H_2O$) and heavy ($D_2O$) water [7].

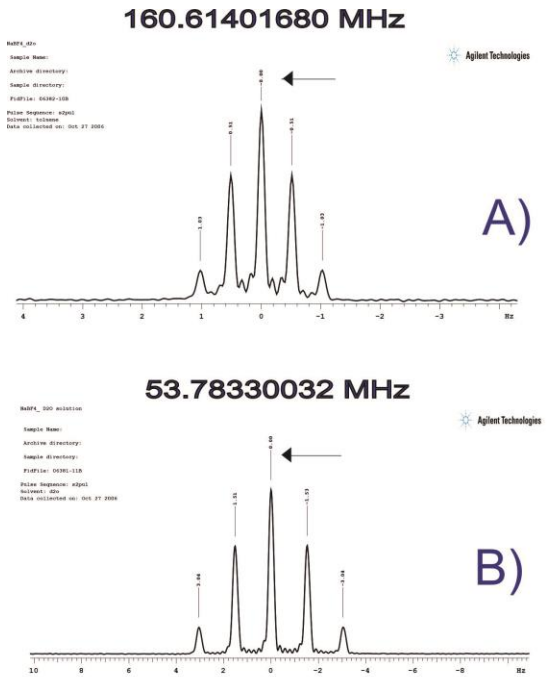



**Figure 5:** A) $^{11}$B NMR ($\Delta_{1/2}$=0.24 Hz), and B) $^{10}$B NMR ($\Delta_{1/2}$~0.12 Hz) spectra of 2.0 mol/L solution of $NaBF_4$ in $D_2O$

### 3.2. Physical Chemistry

It is well known that spectroscopy is a branch of physical chemistry. Here, the chemical shifts and shielding parameters are of prime importance. For NMR spectroscopy, a crucial issue is the referencing of the entire spectrum. In our case, the main problem lies here in the proper referencing of $^{19}$F (and also $^{11}$B or $^{10}$B) NMR

spectra. It can be avoided by measuring references, mainly liquid $CFCl_3$ ($^{19}F$ spectrum) and liquid $BF_3O(C_2H_5)_2$ ($^{11}B$ and $^{10}B$), placed in capillary tubes and inserted into standard 5 mm test tubes with the proper deuterated solvent (e.g., $D_2O$). Figure 6 shows the 470.969 MHz $^{19}F$ NMR spectrum obtained on an Agilent 500 FT spectrometer (formerly a Varian Unity Plus). The fine structure of the $^{19}F$ signal arises from different chlorine-containing isotopomers: $CF^{35}Cl_3$, $CF^{35}Cl_2{}^{37}Cl$, $CF^{35}Cl^{37}Cl_2$, and $CF^{37}Cl_3$. The isotopic shifts observed here are known as secondary effects (IECS), and the observed intensity variations are due to the chlorine isotopic abundances ($^{35}Cl$, 75.77%; $^{37}Cl$, 24.23%) [3]. They are as follows: $^1\Delta^{19}F(CF^{35}Cl_3, CF^{35}Cl_2{}^{37}Cl))$=-0.006 ppm, $^1\Delta^{19}F(CF^{35}Cl_2{}^{37}Cl, CF^{35}Cl^{37}Cl_2))$=-0.006 ppm, and $^1\Delta^{19}F(CF^{35}Cl^{37}Cl_2, CF^{37}Cl_3)$= -0.006 ppm. The difference between primary and secondary isotope effects (in our case) should be discussed briefly with students. The second peak on the left side should be taken as the reference, i.e., 0.00 ppm on the chemical shift scale.

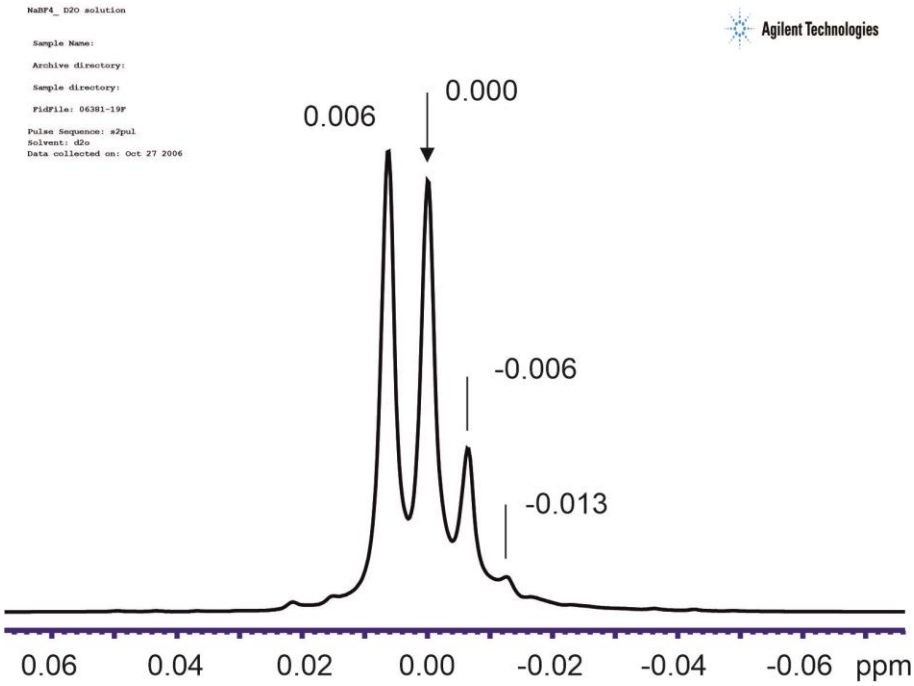



**Figure 6:** $^{19}F$ NMR spectrum of liquid $CFCl_3$. Secondary isotope effects on fluorine nuclei caused by different chlorine compositions are clearly visible

The referencing of entire fluorine and boron spectra in the chemical shift/nuclear magnetic shielding units will be discussed in the next section.

NMR is not a routine method for determining the abundances of different elements. This is mass spectrometry (MS). If possible, it is helpful to measure the mass spectrum of the tetrafluoroborate salt. Fortunately, we have an MS apparatus in our Applicable Laboratory. The given substance is dissolved in methanol and injected into the spectrometer's vacuum chamber (see Appendix 2).

### 3.3. Analytical Questions

The chemical shifts established in the 19F spectrum provided an opportunity to calculate the secondary isotope effect on chemical shift: $^1\Delta\delta^{19}F(^{11}B,^{10}B)$= -0.053 ppm (i.e., 53 ppb). On the other hand, chemical shifts can be transformed to the relative shielding scale or absolute shielding scale (according to Eq.1). The appropriate results can be taken from the absolute shielding of references [8]: $\sigma(^{11}BF_3OEt_2)$=110.9 ppm, $\sigma(^{10}BF_3OEt_2)$ =110.8 ppm, and $\sigma(C^{19}FCl_3)$=192.70 ppm. Susceptibility corrections for water solutions must be taken into account $((-4\pi/3)\chi_V$=+3.006 ppm where $\chi_V = \chi_M\rho/M$). Knowledge of NMR frequencies and shielding corrections enabled calculation of the nuclear magnetic moments of $^{10}B$ and $^{11}B$ relative to $^{19}F$ (NMR method for determining nuclear magnetic moments; see Appendix 4).

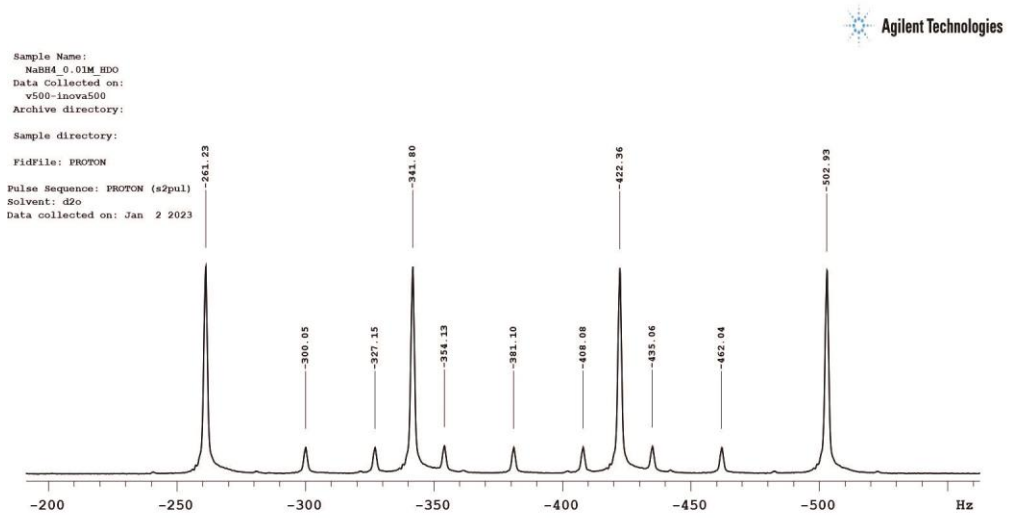



**Figure 7:** $^{1}$H NMR spectrum of solution $NaBH_4$ in heavy water $D_2O$.

Our investigations cannot be limited to the case of tetrafluoroanions; they must also include borohydrides. In the $^{1}$H NMR spectrum presented above (see Figure 7), we can see the 1J(1H,10B) and $^{1}J(^{1}H,^{11}B)$ spin-spin coupling constants. Unfortunately, the secondary isotope effect is almost invisible, with $\Delta^{1}H$ ~0.0025 ppm. On the other hand, the appropriate spin-spin coupling constants are pretty large and easily measurable: $^{1}J(^{1}H,^{11}B) = 80.62$ Hz and $^{1}J(^{1}H,^{10}B) = 27.10$ Hz. Calculating boron abundances from the spectrum presented above is much more complex and requires integrating each individual signal and summing them correctly. The final error would be much higher here than in the former case of the fluorine spectrum.

Warning: dissolving $NaBH_4$ in water can slowly form $NaBO_2$ and gaseous $H_2$ [9]. Very careful handling is needed. The cup cannot grip the NMR test tube tightly. Measurement can be achieved after degassing the sample in the magnetic field, but before final hydrolysis [10]. It requires the teacher to have strong experimental preparation skills.

### 3.4. Nuclear Chemistry

If we record $^{19}$F spectra under full-relaxation conditions for both fluorine signals, good integration can be achieved, and the proper boron isotope abundances can be established: $^{11}$B (80.1%) and 10B (19.9%). It is worth noting that even under adverse magnetic-field conditions, the integration still yields correct results. Analogous results can be received from MS spectra (see Appendix 2). The natural abundances of different elements play an important role in discussions, but $^{11}B/^{10}B$ in minerals and rocks on Earth are in the order of 4:1. The same proportion was found in meteorites and moon rocks - 4.011 ÷ 4.098 [11]. These values primarily represent the Earth's mantle. Nevertheless, the large mass difference between the two isotopes and their high geochemical reactivity can, in some cases, lead to valuable boron isotope fractionation, which becomes a natural process [12]. Observations of element abundances, particularly the light isotopes of hydrogen, lithium, boron, and nitrogen, provide the basis for theories of Solar System formation. The Cosmic Hubble Telescope obtained spectacular measurements of the interstellar gas between Earth and the star δ Scorpii [13]. Valuable discrepancies between galactic cosmic-ray and solar-system abundances of light nuclei suggest different sources for the lithium, beryllium, and boron isotopes, such as stellar nucleosynthesis and neutrino spallation [14]. Interestingly, a few boron-containing chemicals can be enriched in the $^{10}$B or $^{11}$B isotope. For example: boron-$^{10}$B element, tributyl borate-$^{10}$B, boron-$^{10}$B trifluoride, boric acid-$^{11}$B, boron-$^{11}$B oxide, boron-$^{11}$B trifluoride, tributyl borate-$^{11}$B, trimethyl borate-$^{11}$B are offered by the Sigma-Aldrich company.

## 4. Conclusions and Prospects

Finally, we can assume that this simple experimental analysis will be instrumental across various branches of chemistry. Each teacher can make a suitable choice of matter in developing his laboratory exercise. A few modifications to the basic instructions are provided, along with several avenues for extending chemical fields (see Appendices). The experiment described above can be performed using tetrahydroborate salts, e.g., $NaBH_4$ [15]. Unfortunately, the secondary isotope effect is much smaller here, often not measurable, but the spin-spin couplings are much larger. Calculation of abundances requires integrating all 11 signals and summing their areas consecutively. This procedure must, of course, increase the estimation error. In any case, students receive all the basic and advanced information necessary for a general understanding of NMR spectroscopy. Some further consequences of our exercise can be discussed and developed by involving analytical, inorganic, physical, astrophysical, and nuclear puzzles (see Appendices 1, 2, 3, and 4).

Students can prepare their final report after conducting the experiment and analyzing the data. This report should be concise and informative. Each student can note his own remarks and observations. Email the exercise proceedings to the teacher's account.

## Appendix 1.

**NMR pulse sequences** play a crucial role in supporting the spectra. Calibration of the π/2 rectangular pulse is therefore necessary. The 90° pulse-width (pw90) is the length of a pulse that produces the maximum intensity resonance signal. Calibration of the 90° pulse duration is straightforward when a null point can be determined at 180° or 360° pulses. Because relaxation times in $BF_4^-$ solutions are relatively long (a few seconds), the determining pulses require at least one hour. This indicates that it is preferable to record the spectra prior to the experiment. The series of spectra, arranged by pulse width (pw), can be expressed in their usual sinusoidal form. Measurements of T1 relaxation times of signals for $^{10/11}BF_4$ anions can be estimated by the inversion-recovery sequence (d1-π-d2-π/2-fid). The final results indicate T1(11BF4$^-$)=6.05 s and T1($^{10}BF_4^-$) = 8.00 s. The dependence of the signal integration ratio $^{11}B/^{10}B$ as a function of d1 relaxation delay is shown in Figure 8. To achieve proper integration results, a long delay d1 = 30s should be used (9 × T1 for 99.9% integration accuracy).

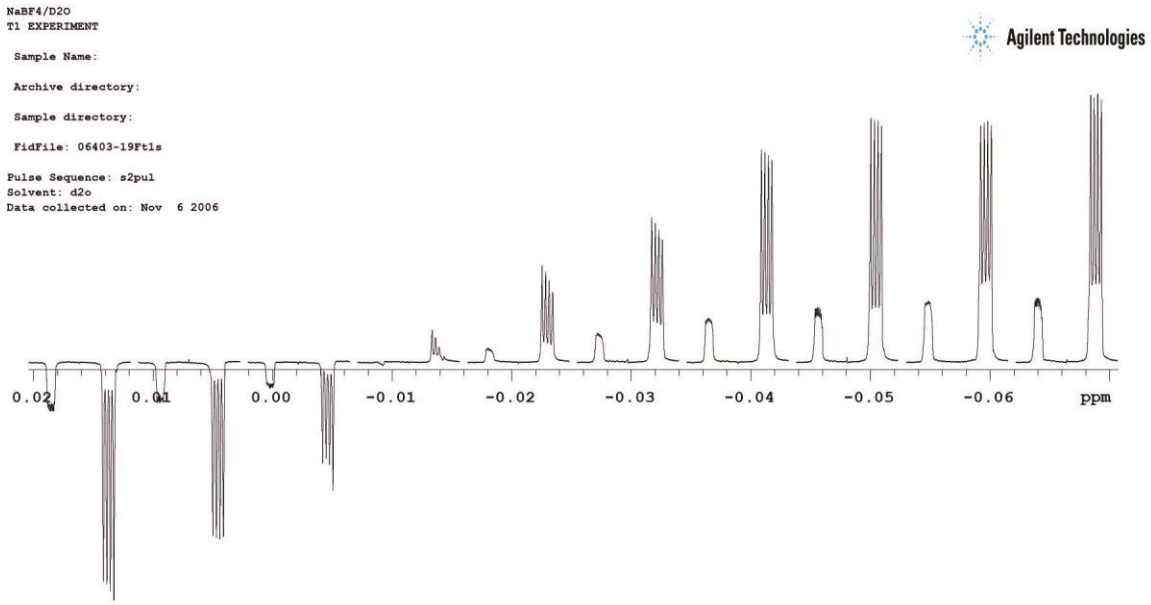



**Figure 8:** $^{19}F$ T1 relaxation time measured by the inversion-recovery method in the tetrafluoroborate anion.

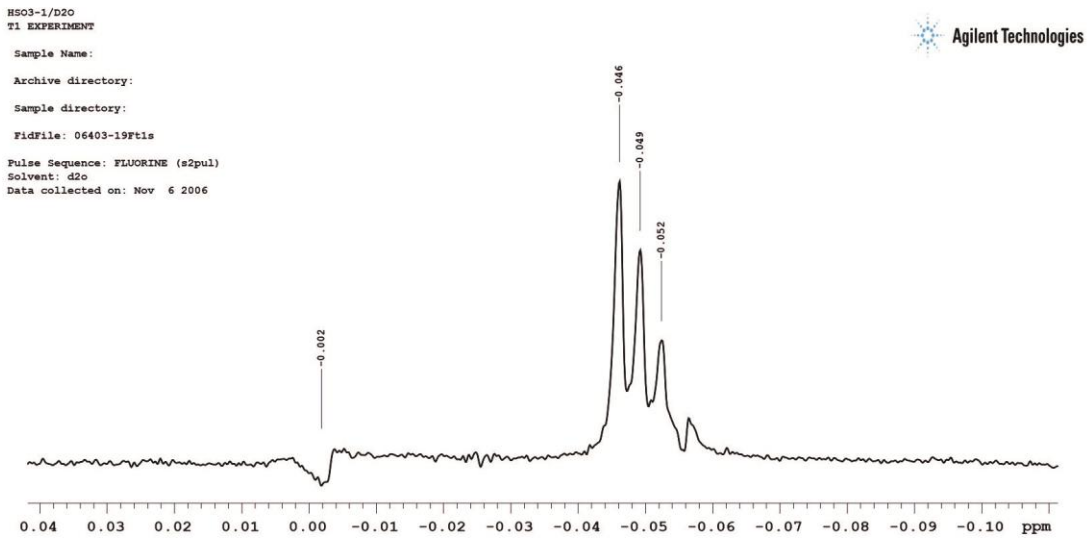



**Figure 9:** One step of the inversion-recovery method for measuring T1 relaxation times of fluorine nuclei in $^{10}BF_4^-$ and $^{11}BF_4^-$ anions. The left signal ($^{10}BF_4^-$) is not yet relaxed (negative), whereas the signal on the right side ($^{11}BF_4^-$) is partially relaxed (positive).

## Appendix 2.

**Mass spectrometry (MS)** is an analytical technique designed to measure the mass-to-charge ratio for anions [16]. A mass spectrum is a plot of intensity as a function of mass-to-charge ratio. This method can be used for alternative measurements of the isotopic composition of $NaBF_4$ [17]. In Figure 10, both the average spectrum (at the top) and the calculated spectrum (at the bottom) are shown.

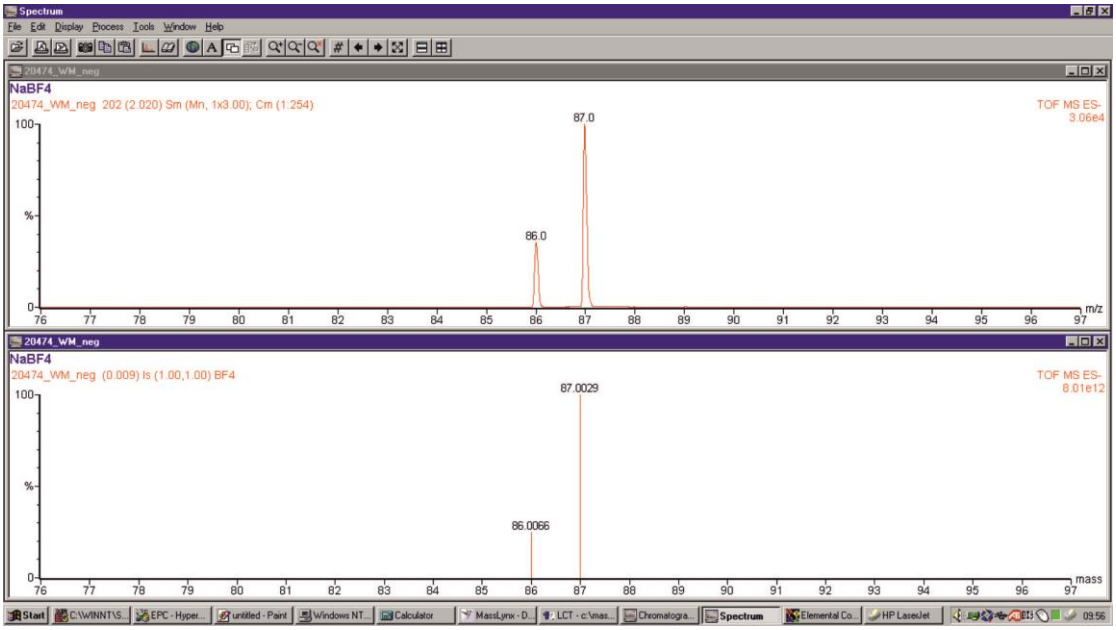



**Figure 10:** Screenshot of $NaBF_4$ MS spectrum. Both tetrafluoroborate signals of anions $^{11}BF_4^-$ and $^{10}BF_4^-$ are visible.

The MS spectrum was recorded on a Micromass LCT mass spectrometer. It is an instrument equipped with an ESI (electrospray ionization) ion source, a TOF (time-of-flight) analyzer, and an MCP (microchannel plate) detector. A solution of the test substance in a polar solvent (e.g., methanol) is injected into the apparatus via a steel capillary, with a voltage applied. The solution is then atomised with an inert gas (nitrogen) and evaporated in the desolvation chamber. Small droplets elsewhere in the apparatus evaporate, and as ions reach the analyser, which, depending on the mass-to-charge ratio (m/z), differentiates their time of flight to the detector. The detector amplifies signals from individual ions, producing processed peaks that are visible in the final spectrum. The $^{11}B/^{10}B$ ratio ~4:1 was confirmed.

Our result is in good agreement with a large number of values found in seawater and Earth's minerals [18].

## Appendix 3.

**Hydrolysis of anions.** It is known that tetrafluoroborate anions in aqueous solutions tend to hydrolyse [19]. This is evident when previously prepared samples are analysed. Within a few days, new anion forms are visible in the 19F and 11B NMR spectra. Students can assume that consecutive reactions take place:

$$BF_4^- + 2H_2O \leftrightarrow BF_3OH^- + F^- + H_3O^+ \ (1)$$

$$BF_3OH^- + 2H_2O \leftrightarrow BF_2(OH)_2^- + F^- + H_3O^+ \ (2)$$

$$BF_2(OH)_2^- + 2H_2O \leftrightarrow BF(OH)_3^- + F^- + H_3O^+ \ (3)$$

$$BF(OH)_3^- + 2H_2O \leftrightarrow B(OH)_4^- + F^- + H_3O^+ \ (4)$$

In NMR investigations, only the first step can be readily observed as $BF_3OH^-$.

The remaining (2), (3), and (4) reactions are too quick to be observed. The NMR timescale matters could be discussed here.

## Appendix 4.

**Nuclear magnetic moments.** If the appropriate radiofrequencies of two different nuclei were measured in the same magnetic field, the nuclear magnetic moments of one of them can be calculated against the second. This is a well-known NMR method for establishing nuclear magnetic moments. In our case, we can simply calculate the $^{11}B$ and $^{10}B$ nuclear moments using the $^{19}F$ nuclear moment as a reference [8,20]. The original results were obtained using a state-of-the-art method performed in the gas phase, but our liquid-phase measurements can also be used [8].

$$\Delta\mu(^{11}B)^z = \frac{160.6140107}{470.9694205} \cdot \frac{0.99966013}{0.99989040} \cdot \frac{\frac{3}{2}}{\frac{1}{2}} \cdot 2.628321 = 2.6883781\mu_N$$

$$\Delta\mu(^{10}B)^z = \frac{53.7340107}{470.96913569} \cdot \frac{0.99966013}{0.99989040} \cdot \frac{3}{\frac{1}{2}} \cdot 2.628321 = 0.8456123\mu_N$$

In the above calculations, the $^{19}F$ nuclear magnetic moment was used as a reference. The spin numbers and the appropriate shielding corrections are included here. They lead to the magnetic moment, defined as the z-component of the full length of the magnetic dipole vector, measured in the superconducting magnet of the NMR spectrometer. Nuclear moments are quoted in nuclear magnetons (n.m. is $5.050783699(31)10^{-27}$ $JT^{-1}$). The difference between the corrected and noncorrected results for shielding effects is ~0.011%. Additionally, the other forms of nuclear magnetic moment units – full-length vector value, gI factor, and gyromagnetic factor $\gamma_I$ - can be discussed, and correlations between them considered.

| $^{10}$B | $^{11}$B | Reference |
|---|---|---|
| 1.8004636(8) | 2.6883781(11) | $^{3}$He [8] |
| 1.8004543(213) | 2.6883642(318) | $^{19}$F [8] |
| 1.8008795 | 2.6889991 | $^{19}$F [this work] (without corrections) |
| 1.8010777 | 2.6892952 | $^{19}$F [this work] (without corrections) |

Table 3: $^{10}$B and $^{11}$B nuclear magnetic moments in $\mu_N$


## Acknowledgement

I am indebted to Dr. Artur Kulesza for technical assistance in conducting the MS measurements.


## References


1. Levitt, M. H. (2008). Spin dynamics: basics of nuclear magnetic resonance. *John Wiley & Sons.*
2. Derome, A. E. (2013). Modern NMR techniques for chemistry research (Vol. 6). *Elsevier*.
3. Braun, S., Kalinowski, H. O., Berger, S., Ernst, L., & Ibrom, K. (1999). 150 and more basic NMR experiments. *Angewandte Chemie-German Edition, 111*(8), 1227-1227.
4. Harris, R. K., Becker, E. D., De Menezes, S. M. C., Granger, P., Hoffman, R. E., & Zilm, K. W. (2008). Further Conventions for NMR Shielding and Chemical Shifts (IUPAC Recommendations 2008) International Union of Pure and Applied Chemistry Physical and Biophysical Chemistry Division. *Magnetic Resonance in Chemistry, 46*(6), 582-598.
5. Kuhlmann, K., & Grant, D. M. (1964). Spin-spin coupling in the tetrafluoroborate ion. *The Journal of Physical Chemistry, 68*(11), 3208-3213.
6. Gillespie, R. J., Hartman, J. S., & Parekh, M. (1968). Solvent effects on the boron–fluorine coupling constant and on fluorine exchange in the tetrafluoroborate anion. *Canadian Journal of Chemistry, 46*(10), 1601-1610.
7. Balz, R., Brändle, U., Kämmerer, E., Köhnlein, D., Lutz, O., & Nolle, A. (1986). $^{11}$B and $^{10}$B NMR investigations in aqueous solutions. *Zeitschrift für Naturforschung A, 41*(5), 737-742.
8. Jackowski, K., Makulski, W., Szyprowska, A., Antušek, A., Jaszuński, M., & Jusélius, J. (2009). NMR shielding constants in BF3 and magnetic dipole moments of $B^{11}$ and $B^{10}$ nuclei. *The Journal of chemical physics, 130*(4).
9. Petit, E., Salles, F., Alligier, D., & Demirci, U. B. (2022). Hydrolysis of the borohydride anion $BH_{4-}$: a $^{11}$B NMR study showing the formation of short-living reaction intermediates including $BH_3OH-$. *Molecules, 27*(6), 1975.
10. Ruman, T., Kuśnierz, A., Jurkiewicz, A., Leś, A., & Rode, W. (2007). The synthesis, reactivity and $^{1}$H NMR investigation of the hydroxyborohydride anion. *Inorganic Chemistry Communications, 10*(9), 1074-1078.
11. Zhai, M., Nakamura, E., Shaw, D. M., & Nakano, T. (1996). Boron isotope ratios in meteorites and lunar rocks. *Geochimica et cosmochimica acta, 60*(23), 4877-4881.
12. Barth, S. (1993). Boron isotope variations in nature: a synthesis. *Geologische Rundschau, 82*(4), 640-651.
13. Federman, S. R., Lambert, D. L., Cardelli, J. A., & Sheffer, Y. (1996). The boron isotope ratio in the interstellar medium. *Nature, 381*(6585), 764-766.
14. De Nolfo, G. A., Yanasak, N. E., Binns, W. R., Cummings, A. C., Christian, E. R., George, J. S., ... & Wiedenbeck, M. E. (2001, November). Measurements of the isotopes of lithium, beryllium, and boron from ACE/CRIS. In AIP Conference Proceedings (Vol. 598, No. 1, pp. 251-255). *American Institute of Physics.*
15. Zanger, M., & Moyna, G. (2005). Measurement of the Isotopic Ratio of $^{10}$B/$^{11}$B in $NaBH_4$ by $^{1}$H NMR. *Journal of chemical education, 82*(9), 1390.
16. Downard, K. (2004). Mass Spectrometry: A Fundation Course, *RSC.*
17. Moraes, M. C., Brito Neto, J. G., & do Lago, C. L. (2001). Boron isotopic ratio by electrospray mass spectra of tetrafluoroboratePart 1. Instrumental conditions, data acquisition, memory effect, and ion stability. *Journal of Analytical Atomic Spectrometry, 16*(11), 1259-1265.
18. Parwel, A., Ubisch, H. V., & Wickman, F. E. (1956). On the variations in the relative abundance of boron isotopes in nature. *Geochimica et Cosmochimica Acta, 10*(3), 185-190.
19. Mesmer, R. E., & Rutenberg, A. C. (1973). Fluorine-19 nuclear magnetic resonance studies on fluoroborate species in aqueous solution. *Inorganic Chemistry, 12*(3), 699-702.
20. Stone, N. J. (2014). Table of nuclear magnetic dipole and electric quadrupole moments. INDC, Vienna, Austria.



***Copyright:*** *©2026 Włodzimierz Makulski, et al. This is an open-access article distributed under the terms of the Creative Commons Attribution License, which permits unrestricted use, distribution, and reproduction in any medium, provided the original author and source are credited.*